Int. J. Environ. Res., 4(4):615-628 , Autumn 2010
ISSN: 1735-6865

Recyclable Rubber Sheets Impregnated with Potassium Oxalate doped TiO_2 and their uses in Decolorization of Dye-Polluted Waters

Suwanchawalit, Ch., Sriwong, Ch. and Wongnawa, S.*

Department of Chemistry and Center for Innovation in Chemistry, Faculty of Science, Prince of Songkla University, Hat Yai, Songkhla 90112, Thailand

Received 12 Aug. 2009; Revised 5 April 2010; Accepted 15 April 2010

ABSTRACT: Two potassium oxalate doped TiO_2 samples, designated as K1-TiO_2 and K2-TiO_2, were synthesized by the base-catalyzed sol-gel process. These samples were impregnated into rubber sheets. Two commercial TiO_2 samples, anatase and Degussa P25, were used as reference materials with which the synthesized samples were to be compared. Anatase and P25 were also impregnated into rubber sheets and designated as Imp-Ana and Imp-P25, respectively. Methylene blue solution was effectively decolorized by these four impregnated sheets. Imp-K1 and Imp-K2 sheets could turn dye solutions to colorless in 3 h and remained at that point until reaching 6h. For the Imp-Ana and Imp-P25 sheets the decolorization rate was slower but increased continually until reaching their maximum at 6h (colorless). The mode of decolorization for the Imp-synthesized TiO_2 was mainly based on adsorption with a small contribution from the photocatalytic reaction while the reverse was observed for the Imp-commercial TiO_2. The surface of the used Imp-synthsized TiO_2 sheets became covered with dye after several uses but it could be cleaned by regeneration with H_2O_2 and UV light. After recycling the cleaned sheets could be reused many times to decolorize the dye solution.

Key words: Immobilized titanium dioxide, Titanium dioxide thin film, Methylene blue, Dye decolorization

INTRODUCTION

Different methods have been utilized in industrial waste treatment for dye decolorization (Sreedhar Reddy and Kotaiah, 2005; Gong et al., 2010; Binupriya et al., 2009; Nagda and Ghole, 2008; Hassani et al., 2008; Nabi Bidhendi et al., 2007). In the field of environmental chemistry, semiconductor mediated photocatalysis has been the focus of recent attention since it aims to destroy contaminants in water and air by non-toxic processes. Following the the pioneering work of Fujishima and Honda in 1972 titanium dioxide (TiO2), has become an important photocatalyst for environmental applications due to its high activity, absence of toxicity, low cost, and excellent durability (Legrini et al.,1993; Lisebigler et al., 1995 and Konstantinou and Albanis, 2004). When TiO2 is irradiated with UV light ($\lambda < 380$ nm), electron–hole pairs are formed which immediately generate free photo electrons and holes that are able to interact with organic matter present at the TiO2 surface. The O2 molecule scavenges an electron from the conduction band of TiO2 to form a superoxide radical (O2") because the energy of the conduction band edge is close to the reduction potential of oxygen. This superoxide reacts with a proton and forms a hydroperoxyl radical (HO2•). These O2" and HO2• species interact with organic pollutants and degrade them to CO2 and water which are harmless products (Houas et al, 2001 and Djaoued et al., 2008). Several studies have dealt with the synthesis of ultrafine TiO_2 nanoparticles and their applications in water purification. However, if used in the powder form, photocatalysts have to be separated from the liquid phase after water treatment and the process for the separation of ultrafine nanoscale particles is tedious and costly (Neppolian *et al*., 2002). The after-used separation process, is one problem that hinders the use of powder photocatalysts to photodegrade toxic or non-biodegradable organic compounds in solution (Zhiyong *et al*., 2008 and Zhiyong *et al*., 2008). These disadvantages could be overcome by using supported photocatalysts for example by fixing TiO_2 on glass (Losito *et al*., 2005), ITO glass (Sankapal and Steiner, 2005), polymer films (Yang *et al*., 2006), and plastic (Kwon *et al*., 2004). TiO_2 thin films have been prepared by various techniques such as chemical vapor deposition (Ding *et al*., 2001), spray pyrolysis deposition (Weng *et al*., 2005), flame synthesis (Partsinis, 1996), and sol-gel dip coating (Sen *et al*., 2005 and Guo *et al*., 2005),however, these techniques need expensive equipment and complex procedures.

*Corresponding author E-mail: sumpun.w@psu.ac.th

In the present study, the synthesized KOX-doped TiO_2 powders (KOX represents potassium oxalate) from our previous work (Suwanchawalit and Wongnawa, 2008) were further exploited by being impregnated into rubber sheets and were investigated for their photocatalytic efficiencies. The advantages of TiO_2 impregnated rubber sheets are that they are more convenient for practical use than TiO_2 in powder form and eliminate the problem of separating TiO_2 powders from water. The synthesized KOX-doped TiO_2 powders were prepared by the sol-gel method, using $TiCl_4$ as the starting material. Hexamethylenetetramine was used as the basic solution to control the rate of hydrolysis and condensation reaction. Potassium oxalate was added in varying amounts: 0.5, 1.0, 2.0, and 4.0 % by mass. Two samples with 0.5 % and 4.0% TiO_2 were selected to impregnate the rubber sheet due to their interesting properties in morphology, surface area, and photocatalytic activity. Their photocatalytic properties were tested by their ability to decolorize methylene blue and compared with commercial Degussa P25 TiO_2 and anatase TiO_2 impregnated rubber sheets prepared in a similar way. The regeneration of the used impregnated rubber sheets and their reusability were also studied.

MATERIALS & METHODS

All chemicals used in this work were of analytical grade and were used without further purification. The main chemicals are commercial titanium dioxide powders (Anatase: AR grade, Carlo Erba, Milano, Italy and P25: Degussa AG, Frankfurt, Germany), titanium tetrachloride ($TiCl_4$, Merck), methylene blue ($C_{16}H_{18}ClN_3S$, Seelze, Germany), potassium oxalate ($(COOK)_2.H_2O$, Ajax Finechem), and hexamethylenetetramine ($C_6H_{12}N_4$, Fluka). Rubber latex (60% HA) was obtained from Chana Latex Co. Ltd., Songkhla, Thailand.

The synthesis of KOX-doped TiO_2 has been described previously (Suwanchawalit and Wongnawa, 2008) and will be mentioned only briefly. $TiCl_4$ (20 mL) was added slowly to 100 mL of cold distilled water to obtain an aqueous solution of titanium tetrachloride. To this solution an appropriate volume of potassium oxalate solution (1.3 M) was added and refluxed at 90 ^oC for 13 h with vigorous stirring. The resulting solution was treated with hexamethylenetetramine to pH 7 and maintained at the same temperature for 13 h. The white precipitate was filtered and washed with distilled water until free of chloride ion by the $AgNO_3$ solution test. The washed samples were dried at 105 °C for a day and ground to a fine powder to give final products designated as *K1-TiO_2* and *K2-TiO_2* for the nominal 0.5 and 4.0 mol% KOX-doped TiO_2, respectively.

Rubber sheets impregnated with TiO_2 powder (designated as Imp-TiO_2) were prepared according to the method described by Sriwong *et al*. (Sriwong *et al*., 2008). For the commercial TiO_2, anatase and P25, the sheets were denoted as *Imp-Ana* and *Imp-P25* for the impregnation of anatase TiO_2 and P25 TiO_2, respectively. They were prepared by mixing 0.1 g of each type of TiO_2 in 3 mL distilled water (in the case of anatase) and in 5 mL distilled water (in the case of P25), stirred for 3 min after which 5 mL of rubber latex (60% HA) was added and then stirred for another 5 min. The mixture was poured into a petri dish (3.5 in. diameter) and left to dry at room temperature for 15 h after which it was taken from petri dish, turned upside down, and dried at room temperature for about another 2 h. The Imp-synthesized TiO_2 sheets were prepared likewise using 0.1 g of the synthesized KOX-doped TiO_2 powders in 1 mL distilled water. They were denoted as *Imp-K1* and *Imp-K2* for the impregnation of K1-TiO_2 and K2-TiO_2, respectively. All the Imp-TiO_2 sheets were tested for stability by submerging the sheets in water and magnetically stirring continuously for 6 h (similar to the decolorization experiments). These sheets did not show any signs of deterioration after the tests. Therefore, all the Imp-TiO_2 sheets prepared by this method could be used in the actual application tests. The crystallization and phase state of the impregnated TiO_2 rubber sheets were studied with the Philips PW 3710 powder diffractometer (PHILIPS X'Pert MPD, the Netherlands) using Cu K_α radiation and equipped with a Ni filter in the range of 5-90° 2θ. The surface features and morphologies of the impregnated TiO_2 rubber sheets were investigated by using a scanning electron micrometer model JSM-5800 LV (JEOL apparatus, Japan). The band gap energies of loose powders and powders impregnated in the rubber sheets were determined using the UV-Vis DRS technique (a Shimadzu UV-2401 spectrophotometer, Shimadzu, Japan).

The photocatalytic activity of the impregnated TiO_2 rubber sheets were tested by decolorization of a methylene blue solution. The experiments were performed in a closed compartment (0.9 m × 0.9 m × 0.9 m) containing 5 fluorescent blacklight (20 W, F20T12-BLB, GE, USA) tubes. The impregnated rubber sheets were placed in a petri dish (10 cm. diameter) containing 50 mL of MB solution (2.5×10^{-5} M) in each experiment. Prior to the illumination, the solution was stirred in the dark for 1 h to reach the adsorption and desorption equilibrium. Then the solution was irradiated using 5 tubes of fluorescence blacklight 20 w (λ_{max} 366 nm) (Randorn *et al*., 2004). In all studies, the solutions were magnetically stirred, before and during illumination. At a given irradiation time interval (every 1 h), 4 mL of

the sample was collected and measured for the remaining concentration of MB by observing the change in absorbance at 665 nm using the UV-Vis spectrophotometer (Specord S100, Analytik Jena GmbH, Germany). The concentration of MB solution was determined quantitatively through the calibration graph constructed from standard solutions of MB at various concentrations ($R^2 = 0.9983$). The percentage of decolorization was calculated by Eq. (1),

$$\% \text{ Decolorization} = \frac{C_0 - C_t}{C_0} \times 100 \quad (1)$$

where C_0 is the initial concentration of MB solution and C_t is the concentration of MB solution at specific time interval for the collected sample. Controlled experiments, without light or without TiO_2, were performed to demonstrate that the degradation of the dye was dependent on the presence of both light and TiO_2.

RESULTS & DISCUSSION

K1-TiO_2 and K2-TiO_2 were synthesized by the sol-gel method and, without calcinations, were impregnated into rubber sheets by the method previously described (Sriwong *et al*., 2008). Prior to the impregnation stage, the loose powders were characterized by XRD and compared with the commercial ones as shown in Fig. 1. For the two commercial TiO_2 samples, anatase and rutile phases are clearly seen, denoted by "A" and "R", respectively. In the synthesized samples, K1-TiO_2 appears to be mainly in its amorphous form with a very small amount of the anatase phase (Fig. 1a); while K2-TiO_2 does not show any characteristic patterns of anatase or rutile but mixed phases of several potassium containing compounds can be observed (Fig. 1b), notably, potassium acetate hydrate ($C_2H_3KO_2.xH_2O$), potassium titanium oxide ($K_2Ti_4O_9$ $2.2H_2O$), and titanium oxide (Ti_3O_5). Some physicochemical properties of K1-TiO_2 and K2-TiO_2 are given in Table 1 including the titanium and potassium contents.

When the loose powders were incorporated into the rubber sheets, the XRD was also used to examine their identities in the new environment and the results are shown in Fig. 2. A well-crystallized anatase form shows up in the Imp-Ana sheet as shown in Fig 2e. The same result is observed for the Imp-P25 sheet as shown in Fig 2d. The pristine rubber sheet shows a clean base line throughout the spectrum except for a

Table 1. Typical physicochemical properties of as-prepared TiO_2 samples

Sample	Crystallite phase	Surface area (m^2/g)	Amount of element	
			Ti[a] (%)	K[a] (%)
K1- TiO_2	Amorphous	336.7	14.08	2.44
K2- TiO_2	Mixed phase*	8.8	7.67	19.55

* Data from XRD: mixed phases are potassium acetate hydrate ($C_2H_3KO_2.xH_2O$), potassium titanium oxide ($K_2Ti_4O_9$ $2.2H_2O$), and titanium oxide (Ti_3O_5).

[a] Determined by XRF using the calibration graph method.

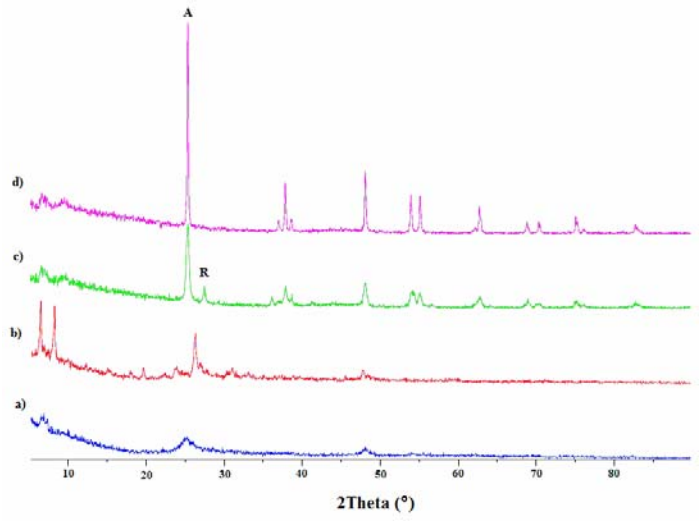

Fig. 1. XRD patterns of TiO_2 powders (a) K1- TiO_2, (b) K2-TiO_2, (c) P25, and (d) anatase.

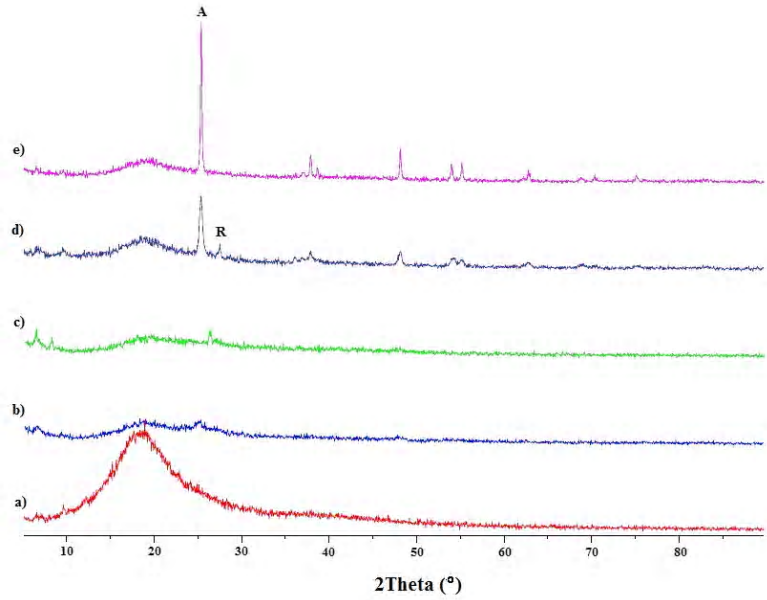

Fig. 2. XRD patterns of (a) pristine rubber sheet, (b) Imp-K1 sheet, (c) Imp-K2 sheet, (d) Imp-Ana sheet, and (e) Imp-P25 sheet.

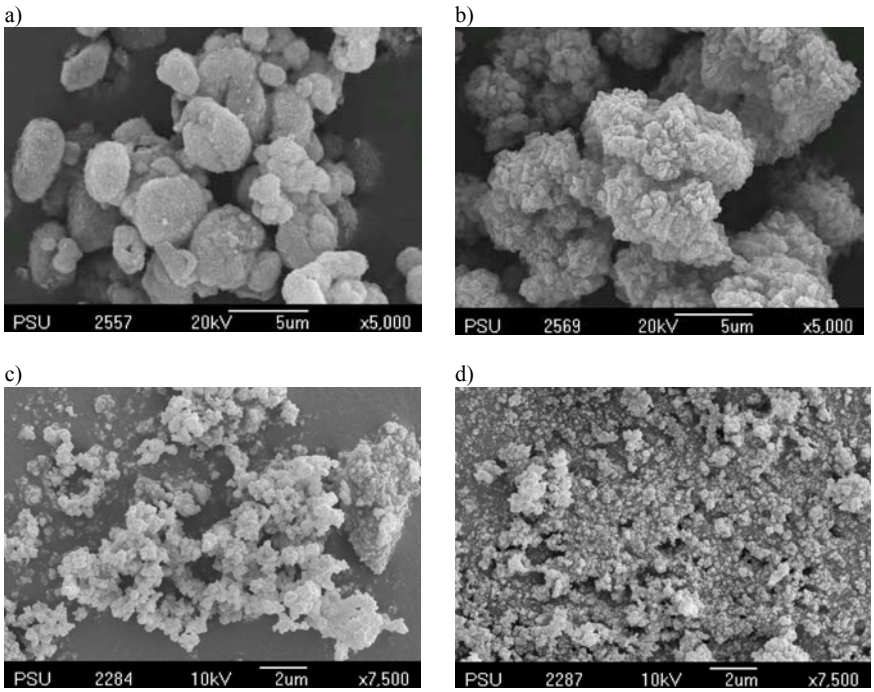

Fig. 3. SEM images of TiO_2 powders (a) K1- TiO_2, (b) K2- TiO_2, (c) Anatase, and (d) P25 Degussa powders.

large broad peak near 2θ = 19 due to scattering of the X-ray beam by the low Z matrix of rubber. This broad scattered peak also shows up in the patterns of both the impregnated sheets but at a much smaller intensity due to the inclusion of TiO_2 particles in the impregnated sheets. The surface with a high content of TiO_2 particles causes the average matrix of the rubber sheet to increase, therefore, there is less scattering of the X-ray beam (Sriwong *et al.*, 2008).

The surface morphology of all Imp-TiO_2 sheets was characterized by scanning electron microscopy (SEM). Figs 3-5 show the SEM micrographs of fresh TiO_2 powders, surfaces of Imp-TiO_2 sheets, and cross-sectional views of Imp-TiO_2 sheets, respectively. Fig 3

shows that TiO_2 loose powders have different morphologies and characteristic properties. The two synthesized samples, K1-TiO_2 and K2-TiO_2, tend to agglomerate into large chunks of particles. K1-TiO_2 is mainly composed of the amorphous phase while K2-TiO_2 has more crystallized phases of potassium titanate compounds readily seen on the surfaces of agglomerated particles. The microstructures of the impregnated rubber sheets, as revealed in Figs 4 and 5, show some significant differences among each of the Imp-TiO_2 sheets. K1-TiO_2 and K2-TiO_2 still remain as large chunks in the rubber matrix and are readily seen on the sheet surfaces. The surface images of Imp-Ana and Imp-K1 sheets are more uniform, with smaller grains, a denser structure and a better surface coverage than the Imp-K2 and Imp-P25 sheets. The sheets were also inspected through cross-sectional views as in Fig. 5. Three sheets, namely, Imp-Ana, Imp-K1, and Imp-K2, show a distinct TiO_2 layer accumulated at the surface. The remaing sheet, Imp-P25, lacks this layer. This can be explained based on the physical property of TiO_2 powders. Loose powders of anatase, K1-TiO_2, and K2-TiO_2, appear as a denser powder than P25. The latter appears as a light and fluffy powder. When these powders were put into the liquid latex the denser ones sank to the bottom faster and accumulated as a layer at the bottom of the dish. When the latex was dry and was removed as a sheet it was *flipped over* such that the bottom surface now became the top surface with the layer of TiO_2 particles on this surface. With this result, we can see that the physical properties of fresh TiO_2 powders, including morphology, particle size, and weight of sample, affected the morphology and efficiency of Imp-TiO_2 rubber sheets. Diffuse reflectance in ultraviolet-visible region was carried out in order to characterize the band gap energy including the nature of electronic transitions in the materials and are shown in Fig. 6. The absorption edge in the UV-Vis DRS was used to calculate the band gap energy by the equation (2);

$$E_g = h\frac{c}{\lambda} \quad (2)$$

where E_g is the band gap energy (eV), h is the Planck's constant, c is the light velocity (m/s), and λ is the wavelength (nm).

The calculated band gap energies of the TiO_2 powder samples and Imp-TiO_2 rubber sheets are shown in Table 2. The band gap energies of the loose powders and the impregnated sheets are almost unchanged. The slight differences could be the result of small errors inherited in the reading of the absorption edge wavelength in the case of the Imp-TiO_2 sheets. The base lines of loose powders are near zero on the absorbance scale while those of the Imp-TiO_2 sheets show

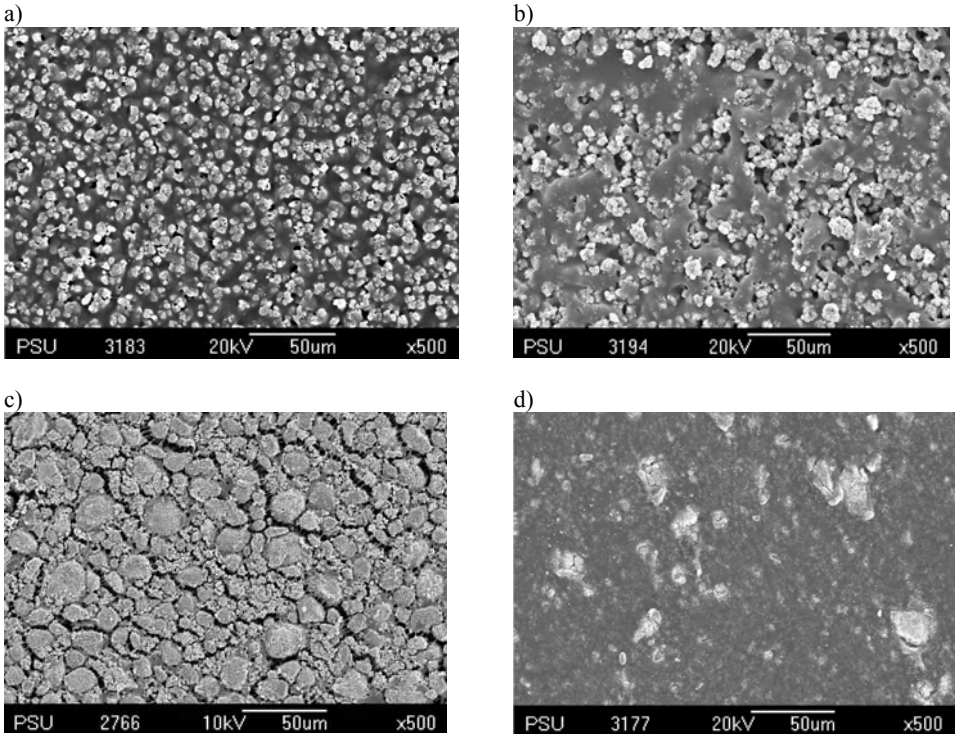

Fig. 4. SEM micrographs of Imp-TiO_2 rubber sheets (a) Imp-K1 sheet, (b) Imp-K2 sheet, (c) Imp-Ana sheet, and (d) Imp-P25 sheet

considerable absorption across the spectral range. This could be attributed to absorption by the rubber matrix. This elevation of base lines made it difficult to extrapolate to obtain an accurate absorption edge wavelength. Nonetheless, the almost unchanged band gap energies in transforming from loose powder to impregnated sheet is not unexpected since the rubber matrix only physically covers the TiO_2 particles, it does not penetrate into the lattice sites to cause some chemical changes.

Methylene blue (MB) was the substrate employed to evaluate the photocatalytic activity of the Imp-TiO_2 rubber sheets. Two blank experiments were performed, one with only the MB solution, the other with a pristine rubber sheet in the MB solution and neither showed any significant change in the color of the MB solutions (or the absorbances in the spectra). This result confirmed that the photocatalytic activity originated from the TiO_2 particles impregnated in the rubber sheet. The detailed mechanism of the photocatalytic oxidation process has been discussed previously in the literatures (Konstantinou and Albanis, 2004;Houas *et al*., 2001; Prevot *et al*., 2001; Tanaka *et al*., 2000; Saien and Khezrianjoo, 2008; Galindo *et al*., 2000; Bandara *et al*., 1999 and Daneshvar *et al*., 2003). Most photocatalytic oxidation processes involve the generation of a very powerful oxidizing agent, the hydroxyl radiacal ($^{\bullet}OH$), that will attack and destroy any organic pollutants. It is well established that when TiO_2 is illuminated with light of $\lambda < 390$ nm, electrons are promoted from the valence band to the conduction band of the TiO_2 to give electron-hole pairs. The valence band hole (h^+_{VB}) is sufficiently strong to generate hydroxyl radicals at the surface and, likewise, for the conduction band

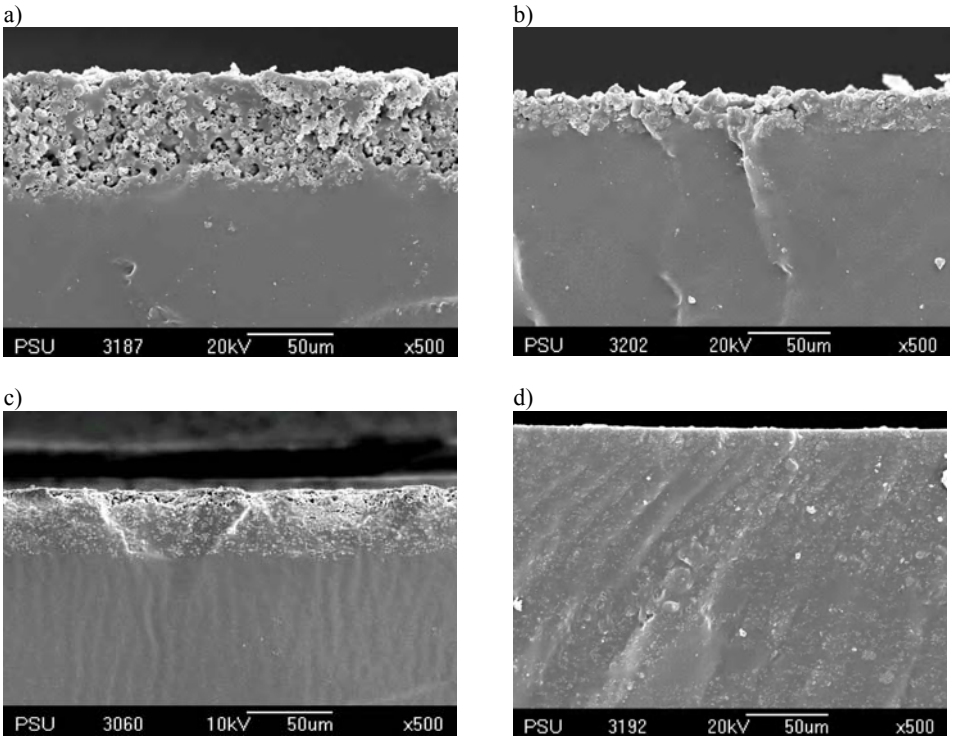

Fig. 5. SEM cross-sectional micrographs of Imp-TiO_2 rubber sheets (a) Imp-K1 sheet, (b) Imp-K2 sheet, (c) Imp-Ana sheet, and (d) Imp-P25 sheet.

Table 2. Band gap energies of TiO_2 samples in the form of powder and Imp-TiO_2 rubber sheets.

Sample	*Imp-TiO_2 rubber sheet*		*TiO_2 powder*	
	λ (nm)	**Band gap energy (eV)**	**λ (nm)**	**Band gap energy (eV)**
P25	400	3.10	392	3.16
Anatase	389	3.19	385	3.22
K1- TiO_2	390	3.18	388	3.20
K2- TiO_2	385	3.22	390	3.18

a) TiO_2 powder DRS spectra

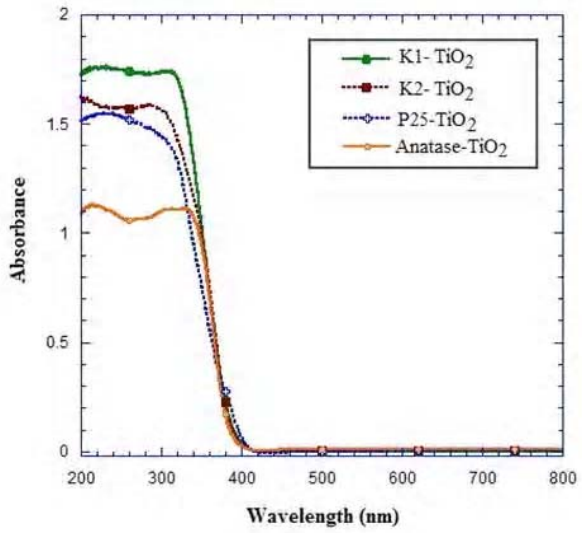

b) Imp-TiO_2 rubber sheet spectra

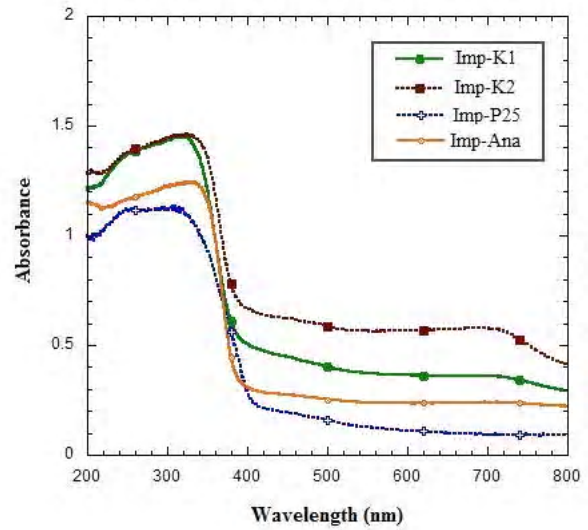

Fig. 6. DRS spectra of a) powder TiO_2 and b) Imp-TiO_2 rubber sheets

electron (e^-_{CB}) to reduce the oxygen molecules to superoxide radicals. The generated hydroxyl radicals are present at the surface of TiO_2 or near to it (within 0-500 μm). The resulting $^{\bullet}OH$ radical can oxidize most of the azo dye to the mineralized end-products. According to this scheme, the relevant reactions at the semiconductor surface causing the degradation of methylene blue can be summarized as follows:

$$TiO_2 + h \rightarrow TiO_2\ (e^-_{CB} + h^+_{VB}) \quad (3)$$
$$h^+_{VB} + e^-_{CB} \rightarrow \text{heat (recombination)} \quad (4)$$
$$h^+_{VB} + H_2O_{(ads)} \rightarrow H^+ + {}^{\bullet}OH_{(ads)} \quad (5)$$
$$h^+_{VB} + OH^-_{(ads)} \rightarrow {}^{\bullet}OH_{(ads)} \quad (6)$$
$$e^-_{CB} + O_{2\,(ads)} \rightarrow O_2^- \quad (7)$$
$$O_2^- + H^+ \rightarrow HO^{\bullet}_2 \quad (8)$$
$$HO^{\bullet}_2 + HO^{\bullet}_2 \rightarrow H_2O_2 + O_2 \quad (9)$$
$$H_2O_2 + h \rightarrow 2\,{}^{\bullet}OH \quad (10)$$
$$H_2O_2 + e^-_{CB} \rightarrow OH^- + {}^{\bullet}OH \quad (11)$$
$${}^{\bullet}OH + \text{dye} \rightarrow \text{degradation of dye} \quad (12)$$
$$h^+_{VB} + \text{dye} \rightarrow \text{oxidation of dye} \quad (13)$$

Fig 7 shows the photocatalytic efficiencies of the prepared Imp-TiO_2 rubber sheets. During the first few hours both the doped TiO_2 sheets (Imp-K1 and Imp-K2) showed greater decolorization efficiencies than the commercial TiO_2 sheets (Imp-P25 and Imp-Ana). The latter pair, however, could catch up with the former pair during the 5th and 6th hours where complete decolorizations were obtained (water was colorless and clear). Inspection of the graphs in Fig. 7 reveals that the doped TiO_2 sheets decolorized the dye solution based primarily on their high adsorptivities in the first hour plus a small contribution from photocatalytic activity during the 2nd – 6th hours. In the case of the commercial TiO_2 sheets, the results are the opposite in that the photocatalytic activity plays a more important role during the same period. In the powder form, the doped TiO_2 samples, K1-TiO_2 and K2-TiO_2, showed high adsorptivity and with this property they could decolorize the dye solution to a clear colorless liquid at a higher efficiency than the commercial powder TiO_2 (P25 and anatase). The same trend, no doubt manifests itself again, when these powders were impregnated into the rubber sheets. The Imp-K1 sheet performed the highest efficiency for decolorization of the methylene blue solution. It is not surprising that the Imp-K1 sheet had a higher efficiency than the Imp-K2 sheet, due to the highly uniform TiO_2 particles distributed on the surface of the Imp-TiO_2 rubber sheet and including the particularly high surface area of the K1- TiO_2 sample. Therefore, the fresh Imp-K1 sheet has higher decolorization efficiency than Imp-K2 sheet and is also higher than both the Imp-Ana and Imp-P25 sheets.

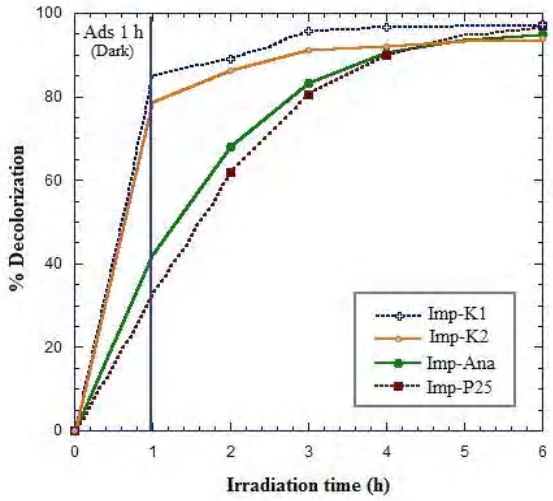

Fig. 7. The decolorization by Imp-TiO_2 rubber sheets (including adsorption).

Kinetics of the photocatalytic oxidation reactions of many organic compounds have often been modeled with the Langmuir-Hinshelwood equation which also covers the adsorption properties of the substrate on the photocatalyst surface (Houas *et al*., 2001; Prevot *et al*., 2001; Tanaka *et al*., 2000; Ibhadon *et al*., 2008 and Chiou *et al*., 2008). The modified L-H equation, where the reaction rate, r, is proportional to the surface coverage, θ, is given by:

$$r = -\frac{dC}{dt} = k_r\theta = \frac{k_r KC}{1+KC} \qquad (14)$$

where k_r is the reaction rate constant, K is the adsorption coefficient of the reactant, and C is the reactant concentration at any time, *t*. When C is very small, KC is negligible with respect to unity and eq. (14) fits to a first order kinetics. The integration of eq. (14) with the limit condition that at the start of radiation, t=0, the concentration is the initial one, $C=C_0$, yields eq. (15):

$$-\ln\left(\frac{C}{C_0}\right) = k_r Kt = k_{app}t \qquad (15)$$

Table 3. The rate constant values of Imp-TiO_2 rubber sheets towards MB degradation.

Imp-TiO_2 rubber sheets	k_{app} (h^{-1})	R^2
Imp-K1	0.3758	0.9768
Imp-K2	0.2902	0.9542
Imp-P25	0.5447	0.9892
Imp-Ana	0.6251	0.9989

$$\ln\left(\frac{C_0}{C}\right) = k_{app}t \qquad (16)$$

where $k_{app} = k_r K$, k_{app} is the apparent first order rate constant. A plot of $\ln(C_0/C)$ versus time represents a straight line, the slope of which upon linear regression equals the apparent first-order rate constant k_{app}.

In the plot of $\ln(C_0/C)$ versus time (Fig 8), all four Imp-TiO_2/rubber sheets showed their straight line behaviour during the period of irradiation (excluding adsorption), indicating that the degradations of methylene blue by these sheets are a first order process. The rate constant values resulting from the application of eq. (16) are summarized in Table 3 for the Imp-TiO_2 rubber sheets.

As the charge of MB molecules and the surface of the TiO_2 photocatalyst are both pH-dependent, so the influence of pH on the decolorization of the dye was studied in the range from 3 to 8 including the natural pH of the MB solution at 6.8. The pH was adjusted by adding an aqueous solution of either HCl or NaOH. Fig 9 shows the effect of pH on the adsorption of dye on the surface of the TiO_2 catalyst and the combined adsorption-photodegradation (or "decolorization") of dye in an aqueous TiO_2 suspension. It is well known that pH would influence both the surface state of titanium and the ionization state of the ionizable dye molecules. The point of zero charge (pzc) of the TiO_2 (Degussa P25) is 6.8 (Konstantinou and Albanis, 2004), thus, the TiO_2 surface is positively charged in acidic media (pH<6.8), whereas it is negatively charged under alkaline condition (pH > 6.8), according to the following reactions (Wen *et al*., 2005):

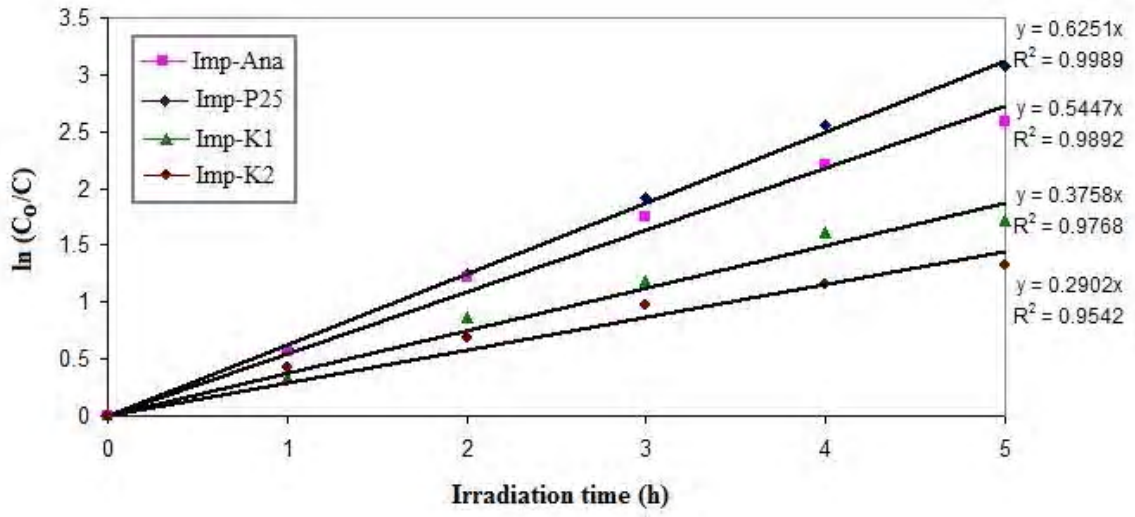

Fig. 8. The kinetics of disappearance of methylene blue by all four Imp-TiO_2 rubber sheets (excluding adsorption prior to irradiation)

$pH < pzc$: $Ti\text{-}OH + H^+ \rightarrow TiOH_2^+$ (17)

$pH > pzc$: $Ti\text{-}OH + OH^- \rightarrow TiO^- + H_2O$ (18)

Since the parent fragment of MB has a positive charge, the adsorption on a negatively charged surface of TiO_2 is favored at high pH. Increasing the pH caused the surface of TiO_2 to become less positive or even turned to negative once the pH exceeded pzc. Hence, we expect that the repulsive force to operate is stronger at low pH, therefore there is less adsorption of dye onto the TiO_2 surface. This fact is borne out as the adsorption trend from pH 3 to 8 of the Imp-TiO_2 sheets gradually increases as shown in Fig 9a. The decolorizations (Fig 9b) also gradually increased when increasing the pH values due to higher concentrations of the •OH radical, hence, the high decolorization efficiencies. So, the order of the efficiency of decolorization by all Imp-TiO_2 rubber sheets at different pH values is pH 8 > pH 6.8 > pH 3.To determine the recyclability of the rubber sheets, all Imp-TiO_2 rubber sheets were used in repeated consecutive photocatalytic runs. After the first round of photocatalytic experiment, the rubber sheet was separated and used in the next round without any treatment. The results in Fig. 10 show that the activity

a) Adsorption

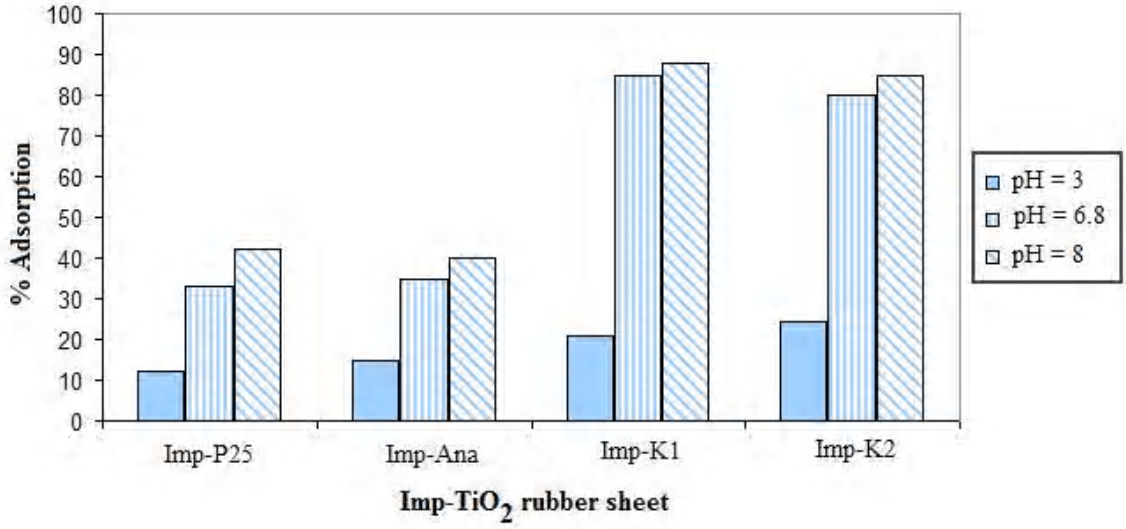

b) Decolorization (adsorption + photodegradation)

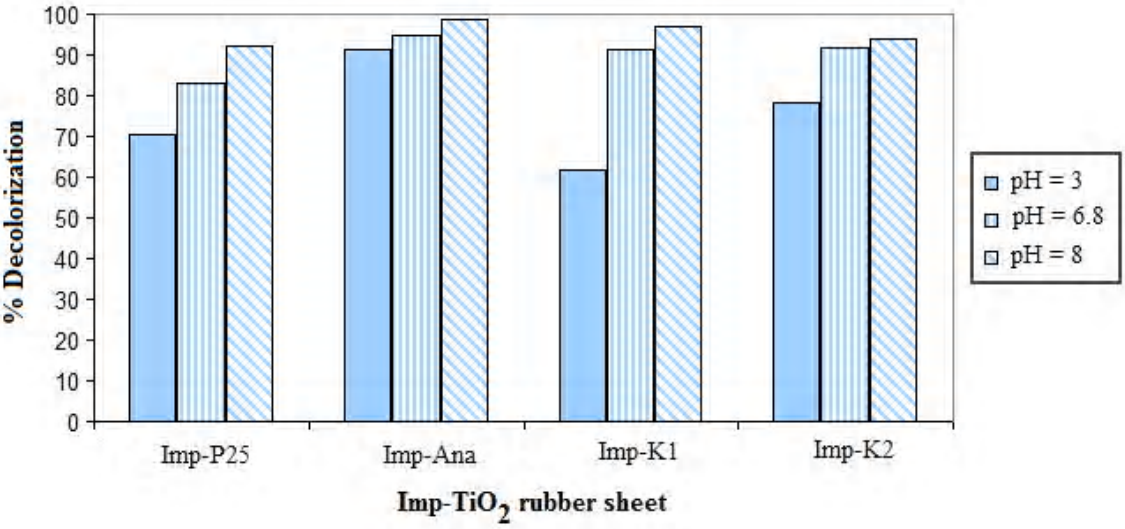

Fig. 9. Effect of pH on a) adsorption of MB on the rubber sheet surface, and b) the combined adsorption-photodegradation of MB by the rubber sheet. (Condition: Imp-TiO_2 sheet , 50 mL MB solution, adsorption in the dark 1 h (a) and under UV irradiation 5 h. (b))

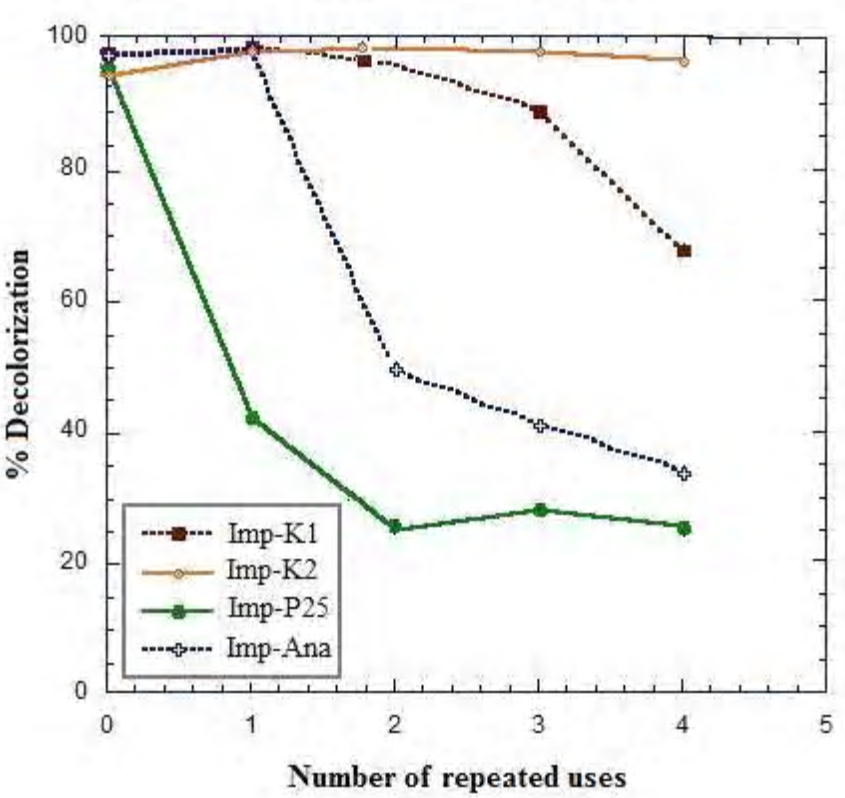

Fig. 10. The efficiencies of MB degradation by Imp-TiO_2 rubber sheets during repeated uses with no cleaning (including adsorption).

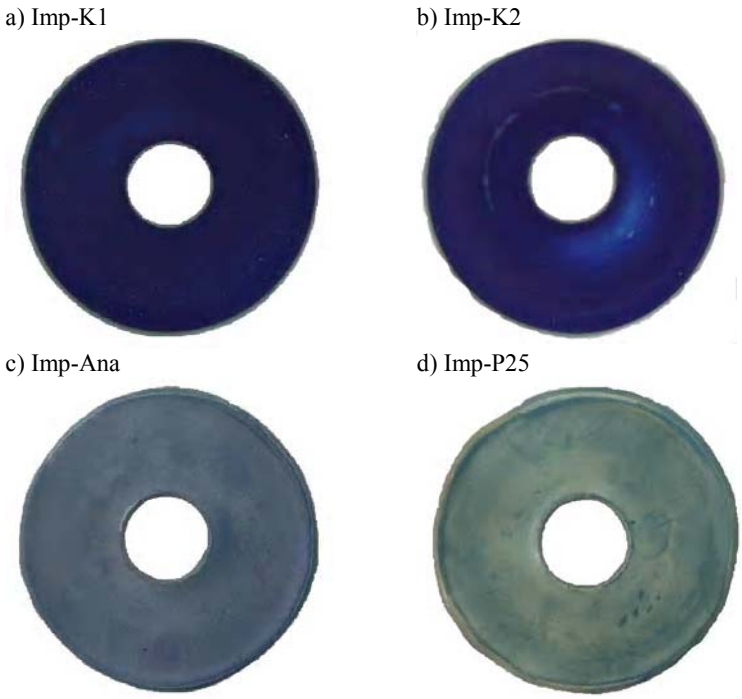

Fig. 11. The photographs after the 4th use of Imp-TiO_2 rubber sheets (without cleaning): (a) Imp-K1 sheet, (b) Imp-K2 sheet, (c) Imp-Ana sheet, and (d) Imp-P25 sheet

of the Imp-commercial TiO_2 rubber sheets decreased greatly in successive uses by up to four times. On the other hand, the activity of the Imp-synthesized TiO_2 rubber sheets decreased only slightly for the Imp-K1 and the Imp-K2 sheet produced excellent performance throughout. When freshly prepared and being used for the first time the Imp-K1 sheet showed a higher photocatalytic efficiency than the Imp-K2 sheet, as shown in Fig 10 (data on the y-axis). However, in the following repeated uses the Imp-K2 sheet maintained

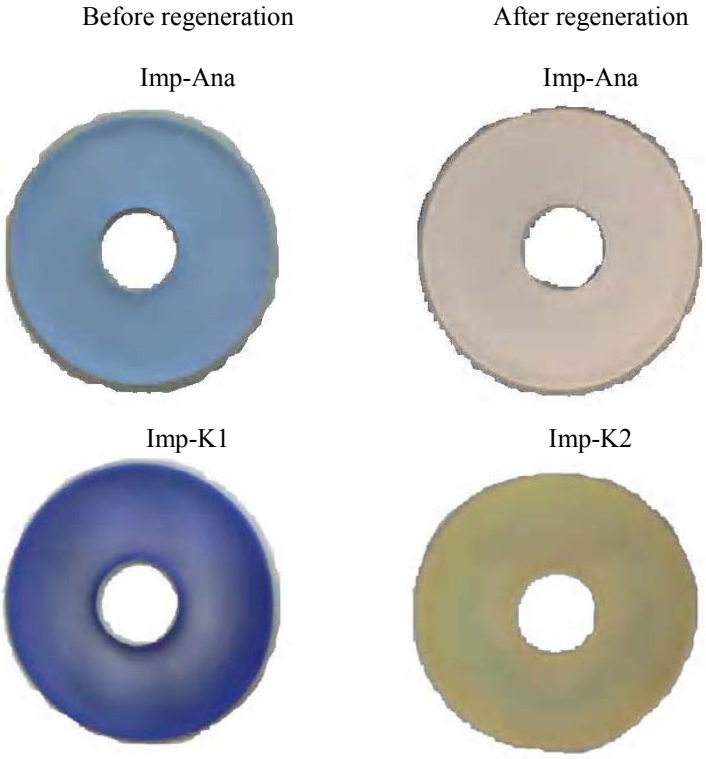

Fig. 12. The photographs of Imp-TiO_2 rubber sheets: before and after regeneration.

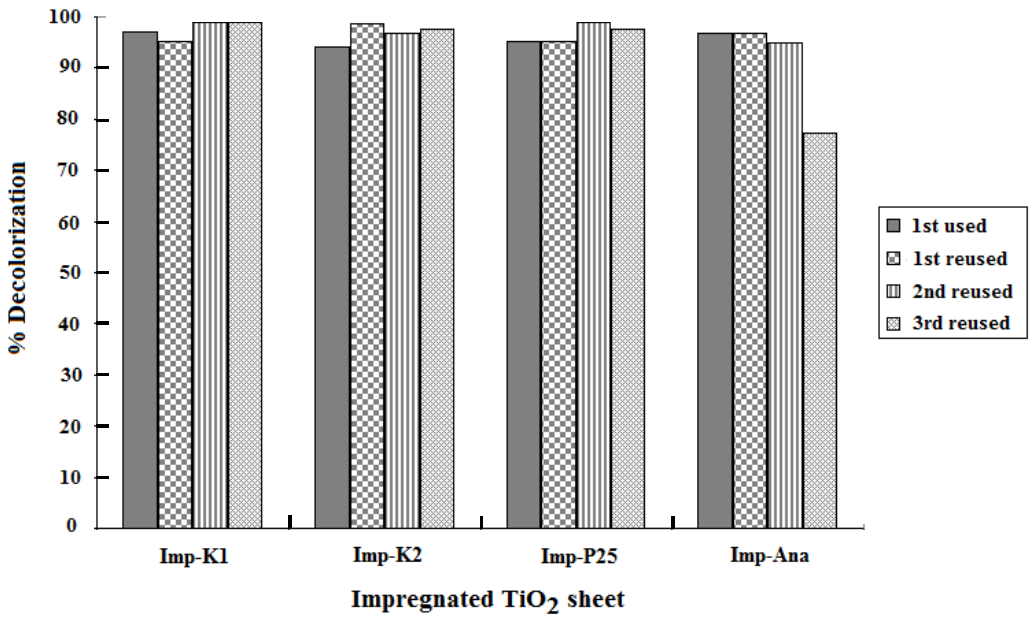

Fig. 13. The efficiencies of MB decolorization by the regenerated Imp-TiO_2 rubber sheets after repeating uses (including adsorption)

its good decolorization efficiency better than the Imp-K1 sheet. These results could be a result of the high adsorption property of the Imp-K1 sheet rendering its surface to be densely covered with methylene blue molecules as shown in Fig 11a (Fig 11 shows photographs of the Imp-TiO_2 rubber sheets (without cleaning) after the 4th use).

After the decolorization experiments, the surfaces of the Imp-TiO_2 rubber sheets were all covered with dye molecules. The clean surface, however, could be regenerated for further uses. The regeneration was carried out by treating the used rubber sheet in 50 mL of H_2O_2 solution (0.2 M) with stirring overnight under UV light irradiation. The regenerated Imp-commercial TiO_2 sheets were off-white and pale yellow for the Imp-synthesized TiO_2 sheets compared with the plain white of the freshly prepared sheets with either commercial or synthesized TiO_2 powder. Photographs of selected Imp-TiO_2 sheets before and after regeneration are shown in Fig.12.

The performances of the two regenerated Imp-TiO_2 sheets were compared to the freshly prepared Imp-TiO_2 sheets (Fig. 13). The sheets regenerated with H_2O_2 had a higher decolorization ability than the freshly prepared TiO_2 rubber sheets.

In the regeneration process, the presence of both H_2O_2 and UV light was necessary to increase the reactive ^{o}OH radicals in the regeneration setup. It appears that H_2O_2 played a major role in destroying the dye molecules previously adsorbed onto the TiO_2 surface. This resulted from the increasing concentration of the ^{o}OH radical according to the following equations (Neppolian *et al*., 2002).

$$H_2O_2 \rightarrow 2\,{}^{o}OH \quad (19)$$

$$H_2O_2 + e^- \rightarrow OH^- + {}^{\bullet}OH \quad (20)$$

$$H_2O_2 + O_2^{\cdot -} \rightarrow OH^- + {}^{\bullet}OH + O_2 \quad (21)$$

Eq (19) represents the homolytic cleavage of H_2O_2 by light while eqs. (20)-(21) are associated with the photocatalytic reaction of TiO_2. The occurrence of $^{\bullet}OH$ in eq. (20) is due to H_2O_2 being reduced by the conduction band electron. The production of $^{\bullet}OH$ from eq. (21) is negligible due to only a small amount of $O_2^{\cdot -}$ anion being produced (Baiju *et al*., 2007). Besides eq. (20), the source of $^{\bullet}OH$ from eq. (19) cannot be overlooked since in our system, the emission wavelength from the fluorescent UV light was 366 nm and this should be sufficient to initiate the production of the $^{\bullet}OH$ radical in the regeneration process.

CONCLUSION

The impregnated TiO_2 rubber sheets were prepared via a simple mixing process between rubber latex and TiO_2 powders. The efficiency for MB degradation as shown by the impregnated commercial TiO_2 sheets was lower than the impregnated synthesized TiO_2 sheets. However, the Imp-K2 sheet has one clear advantage in that it can be reused many times. Here, we have also shown how to cleanse the dirty sheets that became covered by methylene blue molecules by treatment with hydrogen peroxide solution. The cleansed Imp-TiO_2 sheets could be further used for several times. This regeneration process is expected to be applicable for cleansing the surface of other transition metal oxides, and thus will find a use in many applications.

ACKNOWLEDGEMENTS

This research is supported by the Thailand Research Fund through the Royal Golden Jubilee Ph.D. Program (Grant Nos. PHD/0197/2548 and PHD/0003/2550), the Center for Innovation in Chemistry (PERCH-CIC), Commission on Higher Education, Ministry of Education, and the Graduate School-PSU. Sample of Degussa P25 used throughout this work was donated by Degussa AG, Frankfurt, Germany, through its agency in Bangkok, Thailand.

REFERENCES

Baiju, K.V., Shukla, S., Sandhya, K.S., James, J. and Warrier, K.G.K. (2007). Photocatalytic activity of sol-gel-derived nanocrystalline titania. J. Phys.Chem. C **111**, 7612-7622.

Bandara, J., Mielczarski, J. A. and Kiwi, J. (1999). 2. Photosensitized degradation of azo dyes on Fe, Ti, and Al oxides. mechanism of charge transfer during the degradation. Langmuir **15**, 7680-7687.

Binupriya, A.R., Sathishkumar, M., Jung, S.H., Song, S.H. and Yun, S.I. (2009). A Novel Method in Utilization of Bokbunja Seed Wastes From Wineries in Liquid-Phase Sequestration of Reactive Blue 4. Int. J. Environ. Res., 3(1), 1-12.

Chiou, C.H., Wu, C.Y. and Juang, R.S. (2008). Influence of operating parameters on photocatalytic degradation of phenol in UV/TiO_2 process. Chem. Eng. J. **139**, 322-329.

Daneshvar, N., Salari, D. and Khataee, A.R. (2003). Photocatalytic degradation of azo dye acid red 14 in water: investigation of the effect of operational parameters. J. Photochem. Photobiol. A: Chem. **157**, 111-116.

Ding, Z., Hu, X., Yue, P.L., Lu, G.Q. and Greenfield P.F. (2001). Synthesis of anatase TiO_2 supported on porous solids by chemical vapor deposition. Catal. Today. **68**, 173-182.

Djaoued, Y., Thibodeau, M., Robichaud, J., Balaji, S., Priya, S., Tchoukanova, N. and Bates, S.S. (2008). Photocatalytic degradation of domoic acid using nanocrystalline TiO_2 thin films. J. Photochem. Photobiol. A: Chem. **193**, 271–283.

Fujishima, A. and Honda, K., (1972). Electrochemical photolysis of water at a semiconductor electrode, Nature. **238**, 37-38.

Galindo, C., Jacques, P. and Kalt, A. (2000). Photodegradation of the aminoazobenzene acid orange 52 by three advanced oxidation processes: UV/H_2O_2, UV/TiO_2 and VIS/TiO_2 Comparative mechanistic and kinetic investigations. J. Photochem. Photobiol. A: Chem. **130**, 35-47.

Gong, R., Li, N., Cai, W., Liu, Y. and Jiang, J. (2010). á-Ketoglutaric Acid-Modified Chitosan Resin as Sorbent for Enhancing Methylene Blue Removal from Aqueous Solutions. Int. J. Environ. Res., 4(1), 27-32.

Guo, B., Liu, Z., Hong, L., Jiang, H. and Lee, J.Y. (2005). Photocatalytic effect of the sol–gel derived nanoporous TiO_2 transparent thin films. Thin Solid Films. **479**, 310-315.

Hassani, A. H., Seif, S., Javid A. H. and Borghei, M. (2008). Comparison of Adsorption Process by GAC with Novel Formulation of Coagulation – Flocculation for Color Removal of Textile Wastewater. Int. J. Environ. Res., 2(3), 239-248.

Houas, A., Lachheb, H., Ksibi, M., Elaloui, E., Guillard, C. and Herrmann, J.-M. (2001). Photocatalytic degradation pathway of methylene blue in water. Appl.Catal. B: Environ. **31**, 145-157.

Ibhadon, A.O., Greenway, G.M., Yue, Y., Falaras, P. and Tsoukleris, D. (2008). The photocatalytic activity of TiO_2 foam and surface modified binary oxide titania nanoparticles. J. Photochem. Photobiol. A: Chem. **197**, 321-328.

Konstantinou, I.K. and Albanis, T.A. (2004). TiO_2-assisted photocatalytic degradation of azo dyes in aqueous solution: kinetic and mechanistic investigations. Appl. Catal. B: Environ. **49**, 1-14.

Kwon, C.H., Shin, H., Kim, J.H., Choi, W.S. and Yoon, K.H. (2004). Degradation of methylene blue via photocatalysis of titanium dioxide. Mater. Chem.Phys. **86**, 78-82.

Legrini, O., Oliveros, E. and Braun, A.M. (1993). Photochemical processes for water treatment. Chem. Rev. **93**, 671-698.

Linsebigler, A.L., Lu, G. and Yates, J.T. (1995). Photocatalysis on TiO_2 surfaces: principles, mechanisms, and selected results. Chem. Rev. **95**, 735-758.

Losito, I., Amorisco, A., Palmisano, F. and Zambonin, P.G. (2005). X-ray photoelectron spectroscopy characterization of composite TiO_2 –poly(vinylidenefluoride) films synthesised for applications in pesticide photocatalytic degradation. Appl. Surf. Sci. **240**, 180-188.

Nabi Bidhendi, Gh. R., Torabian, A., Ehsani, H., Razmkhah, N. and Abbasi, M. (2007). Evaluation of Industrial Dyeing Wastewater Treatment with Coagulants. Int. J. Environ. Res., **1(3),** 242-247.

Nagda, G. K. and Ghole, V. S. (2008). Utilization of Lignocellulosic Waste from Bidi Industry for Removal of Dye from Aqueous Solution. Int. J. Environ. Res., 2(4), 385-390.

Neppolian, B., Sakthivel, S., Phalanichamy, M. and Arabindoo, B. (2002). Solar/UV-induced photocatalytic degradation of three commercial textile dyes. J. Hazardous Mater. B. **89**, 303-317.

Neppolian, B., Choi, H.C., Sakthivel, S., Arabindoo, B. and Murugesan, V. (2002). Solar light induced and TiO_2 assisted degradation of textile dye reactive blue 4 Chemosphere, **46**, 1173-1181.

Partsinis, S.E. (1996). Flame synthesis of nanosize particles: precise control of particle size. J. Aerosol Sci. **27**, s153-s154.

Prevot, A.B., Baiocchi, C., Brussino, M.C., Pramauro, E., Savarino, P., Augugliaro, V., Marc, G. and Palmisano, L. (2001). Photocatalytic degradation of acid blue 80 in aqueous solutions containing TiO_2 suspensions. Environ. Sci. Technol. **35**, 971-976.

Randorn , C., Wongnawa , S. and Boonsin, P. (2004). Bleaching of methylene blue by hydrated titanium dioxide. ScienceAsia. **30**, 149-156.

Sankapal, S.B.and Steiner, M.Ch. (2005). Synthesis and characterization of anatase-TiO_2 thin films. Appl. Surf. Sci. **239**, 165-170.

Saien, J. and Khezrianjoo, S. (2008). Degradation of the fungicide carbendazim in aqueous solutions with UV/TiO_2 process: Optimization, kinetics and toxicity studies. J. Hazardous Mater. **157**, 269-276.

Sen, S., Mahanty, S., Roy, S., Heintz, O., Bourgeois, S. and Chaumont, D. (2005). Investigation on sol–gel synthesized Ag-doped TiO_2 cermet thin films.Thin Solid Films. **474**, 245-249.

Sreedhar Reddy, S. and Kotaiah, B. (2005). Decolorization of simulated spent reactive dye bath using solar / TiO2 / H2O2. Int. J. Environ. Sci. Tech., 2(3), 245-251.

Sriwong, C., Wongnawa, S. and Patarapaiboolchai, O. (2008). Photocatalytic activity of rubber sheet impregnated with TiO_2 particles and its recyclability. Catal. Comm. **9**, 213-218.

Suwanchawalit, C. and Wongnawa, S. (2008). Influence of calcination on the microstructures and photocatalytic activity of potassium oxalate-doped TiO_2 powders. Appl Catal A: Gen. **338**, 87-99.

Tanaka, K., Padermpole, K. and Hisanaga, T. (2000). Photocatalytic degradation of commercial azo dyes. Wat. Res. **34**, 327-333.

Wen, B., Liu, C. and Liu, Y. (2005). Optimization of the preparation methods: Synthesis of mesostructured TiO_2 with high photocatalytic activities J. Photochem. Photobiol. A: Chem. **173**, 7-12.

Weng, W., Ma, M., Du, P., Zhao, G., Shen, G., Wang, J. and Han, G. (2005). Superhydrophilic Fe doped titanium dioxide

thin films prepared by a spray pyrolysis deposition. Surf. Coat. Tech. **198**, 340-344.

Yang, J.H., Han, Y.S. and Choy, J.H. (2006). TiO_2 thin-films on polymer substrates and their photocatalytic activity. Thin Solid Films. **495**, 266-271.

Zhiyong, Y., Laub, D., Bensimon, M. and Kiwi, J. (2008). Flexible polymer TiO_2 modified film photocatalysts active in the photodegradation of azo-dyes in solution. Inorg. Chim. Acta. **361**, 589–594.

Zhiyong, Y., Keppner, H., Laub, D., Mielczarski, E., Mielczarski, J., Kiwi-Minsker, L., Renken, A. and Kiwi, J. (2008). Photocatalytic discoloration of Methyl Orange on innovative parylene–TiO_2 flexible thin films under simulated sunlight. Appl.Catal. B: Environ. **79**, 63-71.